



Usak University

Journal of Engineering Sciences

An international e-journal published by the University of Usak

Journal homepage: dergipark.gov.tr/uujes



Research article

SYNTHESIS, STRUCTURAL AND LUMINESCENCE PROPERTIES OF PEG/PVP BLEND POLYMER FILMS CONTAINING Er³⁺ DOPED CeO₂

Kubra Nur Kavas¹, Mustafa Burak Coban^{2*}

¹Department of Physics, Graduate School of Natural and Applied Sciences, University of Balikesir, Türkiye

²Department of Physics, University of Balikesir, Türkiye

Received: September 10, 2024 Revised: October 24, 2024 Accepted: October 24, 2024 Online available: December 30, 2024

Abstract

In this study well-blended Erbium: Cerium oxide doping polyethylene/ polyvinylpyrrolidone blended polymer films were synthesized using a simple solution casting synthesis approach. The changes in crystallization behavior, and luminescence and structural properties of polyethylene glycol and polyvinylpyrrolidone with the addition of cerium oxide and erbium ion have been investigated through FT-IR spectroscopy, X-ray diffraction and luminescence properties. The results show that adding the proper amount of CeO₂:Er³⁺ nanoparticles can play the role of the further nano-filler, which is beneficial to improve the luminescence of blended oxide film. This study contributes to the understanding of the role of interfacial sites in metal and oxide support in blended films for the development of fertile luminescence materials.

Keywords: PEG/PVP blended film; CeO₂:Er³⁺; Photoluminescence; Solution casting method.

©2024 Usak University all rights reserved.

1. Introduction

Recently, versatile polymeric materials have become a part of polymers with strong electronic, optical and structural properties, well-organized geometric strength, strong weathering and fatigue strength, permanently suitable for high temperatures [1–4]. In this context, Polymer bonding or blends of polymers are a class of engineering compounds identical to hybrid structures designed by mixing at least two polymers with enhanced properties to produce a distinct composition with versatile characters [5,6]. Polymer materials blended with nano-fillers or doping polymers have become the focus of many studies in terms of improving the properties of inorganic ingredients and polymer matrices [7,8]. Polyethylene glycol (PEG) has exceptional water solubility, low toxicity and high

*Corresponding author: Mustafa Burak Coban
E-mail: burakcoban@balikesir.edu.tr

DOI: 10.47137/uujes.1547078

©2024 Usak University all rights reserved.

adsorption resistance. On the other hand, As a water-solubility polymer, Polyvinylpyrrolidone (PVP) has sophisticated features such as biodegradability, good dielectric constant, low toxicity, and biocompatibility [9,10].

The lanthanide series of the periodic table begins with the element Cerium, which has the electronic configuration $[Xe], 4f^1, 5d^1, 6s^2$. The 5p and 4d electrons adequately shield the 4f orbitals of the lanthanide, giving them important optical and catalytic properties. In addition, cerium oxide, which has a structure similar to fluorite, can be rapidly oxidized in the air atmosphere even after a significant amount of oxygen loss. Cerium oxide, which crystallizes in a fluorite-like structure, is among the important semiconductor oxides with a band gap between 2.6 and 3.4 eV [11–14].

Furthermore, cerium oxide (CeO_2), because of its excellent high oxygen mobility, hardness index, uv-radiation absorbing-emitting ability, and stability at high temperatures [15,16], plays an important role in many technological fields, such as gas sensors, catalyst support and promoter and glass polishing material [17–19]. Trivalent lanthanide ions such as Yb^{3+} , Ho^{3+} , Tm^{3+} and Er^{3+} contribute to the energy absorption and (or) luminescence centers in these materials. Among these rare earth ions, Er^{3+} is one of the most favourite and efficient luminescent ions. It exhibits emission peaks of three different colors in the visible region range of the electromagnetic spectrum, assigned as blue, green and red light emissions, respectively. Among these luminescence transitions the most important is $^4I_{13/2} \rightarrow ^4I_{15/2}$ erbium emission, which is related to NIR emission, because the spectral range at about 1.53 μm that is the safety for human eyes [20]. In this region, Er^{3+} employs effective roles for optical architectures in telecom infrastructures [21].

Based on this point, in this work, doped nanofiller CeO_2 with Er^{3+} ions PEG/PVP: CeO_2 : Er^{3+} blended polymer films were synthesized using precipitation method and solution casting method, respectively. The effect of nanofiller doped at different rates with Er^{3+} on the structure, and luminescence properties of PEG/PVP blended films was investigated.

2. Materials and Method

The materials used for the study were cerium nitrate hexahydrate ($Ce(NO_3)_3 \cdot 6H_2O$), erbium nitrate pentahydrate ($Er(NO_3)_3 \cdot 5H_2O$), Poly(ethylene glycol) (PEG) (molecular weight 4000), Polyvinylpyrrolidone (PVP) (average molecular weight $\sim 1,300,000$) and sodium hydroxide (NaOH) purchased from Sigma Aldrich.

2.1 Synthesis of CeO_2 and Er doped CeO_2 nanoparticles

The CeO_2 were synthesized precipitation method using $Ce(NO_3)_3 \cdot 6H_2O$ as a precursor. The concentration of Er^{3+} is adjusted to be 1-5 wt.% concerning the Ce^{3+} content in the solution. Then 0.2 M solution of NaOH was prepared to act as a precipitation agent. The 0.2 M solution of NaOH was added to 0.1 M solution of $Ce(NO_3)_3 \cdot 6H_2O$ to achieve the pH value of 7 and continuous stirring for 4 h at 80 °C. The nanostructures were washed with de-ionized (DI) water and ethanol. After that, the product was centrifuged and repeated three times. Finally, they are dried and crushed and oven-dried at 80 °C overnight. Eventually, the prepared material was calcined at 450 °C for 3 h to obtain the yellow-colored CeO_2 . The CeO_2 nanocomposites are formed by using the same method. The dosage of doped $Er(NO_3)_3 \cdot 6H_2O$ are 1-5 wt.%, which are denoted as 1% Er^{3+} - CeO_2 , 2% Er^{3+} - CeO_2 , 3% Er^{3+} - CeO_2 , 4% Er^{3+} - CeO_2 and 5% Er^{3+} - CeO_2 , respectively.

2.2 Synthesis of CeO₂:Er³⁺ (x wt.%) decorated PEG/PVP blend polymer films

The blend polymer films with similar ratios of dopant were blended by performing the solution casting technique to determine the effect on the host polymer blend. The blended films were designed with two polymers: PEG and PVP. Firstly, 0.5 g of PEG with 20 ml of (DI) water, and 0.5 g of PVP with 20 ml were mixed. Secondly, every type was completely provided for solubility. Thirdly, the PEG and PVP polymers were mixed at room temperature for 1 h to get the PEG/PVP homogeneous solution. In a separate beaker, the same weight from (0.5 g) with 10 ml of the CeO₂:xEr³⁺ (x=0, 1, 2, 3, 4 and 5 wt.%) nanoparticles were sonicated for two hours. After that, the blended polymer solution and nanoparticles solution were mixed by the magnetic stirrer for three hours. The pure polymer matrix and CeO₂:xEr³⁺ doped polymer matrix were positioned in Petri dishes, as illustrated in Fig. 1. It was then left to dry in a drying oven at around 40 °C for a maximum of three days.

Finally, the undoped and CeO₂:xEr³⁺-doped PEG/PVP hybrid polymer films were prepared. The names of CeO₂:xEr³⁺ (x=0-5wt.%) doped PEG/PVP hybrid films are determined as PP (PEG/PVP), PPC (PEG/PVP:CeO₂), PPCE1 (PEG/PVP:CeO₂:Er³⁺ (1wt.%)), PPCE2 (PEG/PVP:CeO₂:Er³⁺ (2wt.%)), PPCE3 (PEG/PVP: CeO₂:Er³⁺ (3wt.%)), PPCE4 (PEG/PVP: CeO₂:Er³⁺ (4wt.%)) and PPCE5 (PEG/PVP: CeO₂:Er³⁺ (5wt.%)), respectively. Also, the mean thickness of the as-prepared blended films was recorded to be about 0.000233m.

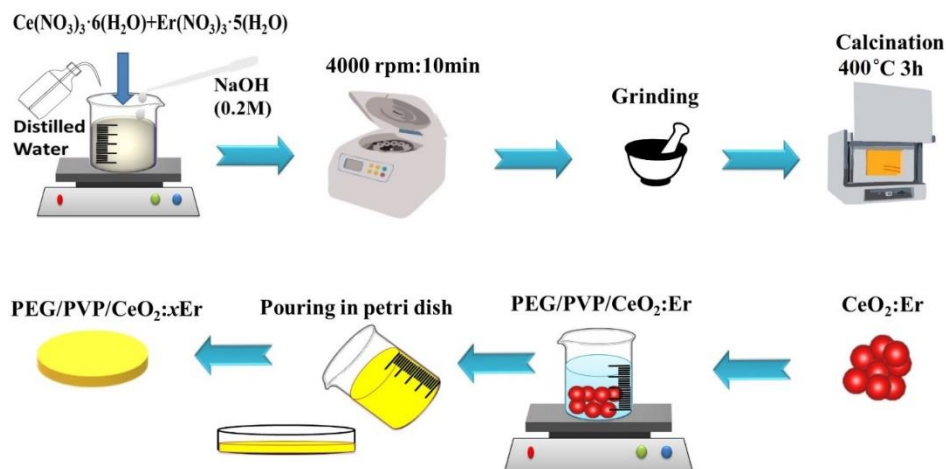


Fig. 1 Preparation of PEG/PVA/CeO₂:xEr³⁺ blend films.

3. Results and discussion

3.1 XRD analysis

The XRD pattern of the pristine-CeO₂ sample is presented in Fig. 2 and Table 1. All the diffraction peaks comply with the JCPDS file for CeO₂ (JCPDS 98-005-4342), which can be assigned to the cubic structure of CeO₂. The JCPDS standard 98-005-4342 with peaks observed at 28.53°, 33.02°, 47.50°, 56.28°, 59.11°, 69.40°, 76.71° and 79.10° assigned to (111), (002), (022), (113), (222), (004), (133) and (024) planes respectively. The pure PP (PEG/PVP) blended film was in good agreement with published literature [22].

The XRD patterns of pure PEG/PVP blend showed one broad peak at $2\theta = 13.15^\circ$ and sharp diffraction peaks at $2\theta = 19.15^\circ$ and 23.43° . This includes most importantly informing the amorphous-crystalline nature of blends. The broad peak indicates the amorphous nature of the PVP, while sharp diffraction peaks originate in the crystalline phase of PEG. This indicates that the feature between the amorphous and crystalline nature of the blended film indicates good miscibility of the two polymers [23,24]. Especially, as the doping rate increases (from PPCE1 to PPCE5), PEG peak intensities drastically decrease. PEG peak intensities are drastically decreased. This formation can be attributed to the fact that chain scission and cross-linking occur.

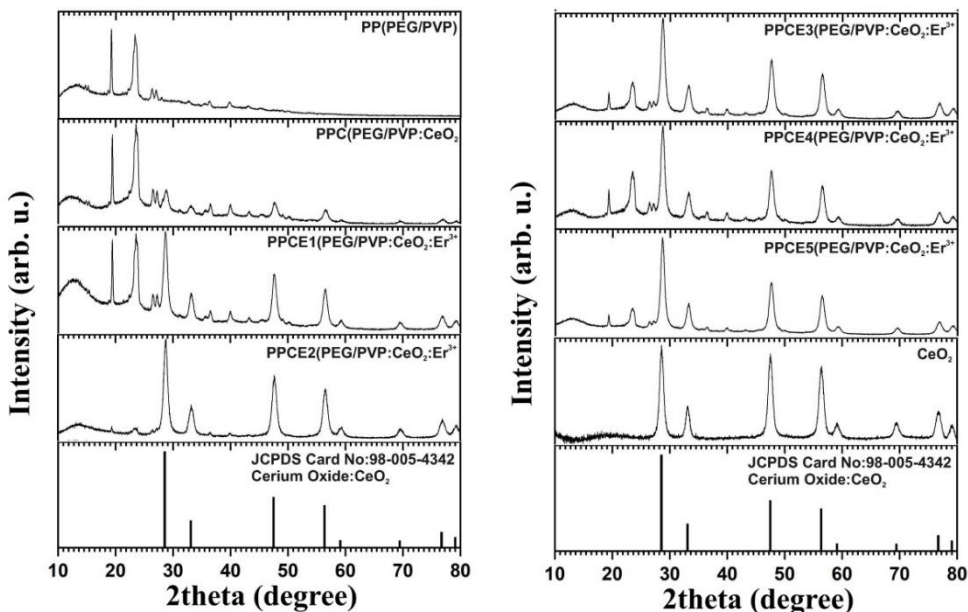


Fig. 2 Powder X-ray diffraction (XRD) patterns of pristine-CeO₂, PEG/PVP:CeO₂ and PEG/PVP:CeO₂:Er³⁺(1-5wt.%).

The crystallite sizes of the pristine-CeO₂ powder and PEG/PVP:CeO₂:Er³⁺(1-5wt.%) blended films are calculated using the Scherer equation:

$$D = 0.9 \lambda / (\beta \cos \theta) \tag{1}$$

where D is crystallite size, λ is the wavelength of the X-rays, β is the full width at a half-maximum intensity of the peaks, and θ is the diffraction angle [25]. Calculations showed that pure CeO₂ particles have a crystallite size of 11.76 nm, while PEG/PVP:CeO₂:Er³⁺ (1wt.%) decreased slightly to 8.45 nm. In the case of the doping rate increases, the crystallite sizes increased slightly to 10.75 nm. It is speculated that the differences in crystallite sizes may result from the aggregation of CeO₂:Er³⁺ nanoparticles, as the PEG/PVP capping agent layers can reduce particle agglomeration and stabilize nanoparticle dispersions.

Table 1 Particle size estimated from the diffraction spectrum of pristine-CeO₂, PEG/PVP:CeO₂ and PEG/PVP:CeO₂:Er³⁺(1-5wt.%) by using FWHM.

Pos. [2θ°]	FWHM [2θ°]	d-spacing [Å]	Particle size(PS)	Av. PS	Pos. [2θ°]	FWHM [2θ°]	d-spacing [Å]	Particle size(PS)	Av. PS
CeO₂					PEG/PVP:CeO₂:Er³⁺(3wt.%) (PPCE3)				
28.52	0.90	3.13	9.14	11.76	28.67	0.96	3.11	8.55	9.00
33.07	0.73	2.71	11.29		33.21	0.96	2.70	8.64	
47.47	0.90	1.91	9.67		47.61	0.77	1.91	11.31	
56.32	1.06	1.63	8.50		56.49	0.96	1.63	9.40	
59.06	0.82	1.56	11.19		59.19	1.15	1.56	7.93	
69.38	0.82	1.35	11.84		69.54	1.15	1.35	8.40	
76.61	0.49	1.24	20.68		76.82	1.15	1.24	8.80	
PEG/PVP:CeO₂ (PPC)					PEG/PVP:CeO₂:Er³⁺(4wt.%) (PPCE4)				
28.62	0.86	3.12	9.49	11.24	23.42	0.86	3.79	9.39	10.37
33.14	0.77	2.70	10.80		28.68	0.53	3.11	15.54	
47.54	0.86	1.91	10.05		33.19	0.96	2.70	8.64	
56.42	0.67	1.63	13.42		47.58	0.86	1.91	10.05	
59.18	0.86	1.56	10.58		56.43	0.77	1.63	11.74	
69.46	0.77	1.35	12.59		69.48	1.15	1.35	8.39	
76.81	0.86	1.24	11.74		76.79	1.15	1.24	8.80	
PEG/PVP:CeO₂:Er³⁺(1wt.%) (PPCE1)					PEG/PVP:CeO₂:Er³⁺(5wt.%) (PPCE5)				
23.58	0.86	3.77	9.40	8.45	28.63	0.53	1.24	15.53	10.75
26.75	1.15	3.33	7.09		33.15	0.67	1.24	12.34	
28.76	0.96	3.10	8.55		47.55	0.86	1.24	10.05	
36.17	1.15	2.48	7.26		56.40	0.86	1.24	10.44	
39.98	1.15	2.25	7.34		59.13	1.15	1.24	7.93	
47.64	0.96	1.91	9.05		69.46	1.15	1.24	8.39	
56.48	0.86	1.63	10.44		76.82	0.96	1.24	10.56	
PEG/PVP:CeO₂:Er³⁺(2wt.%) (PPCE2)									
28.70	0.86	3.11	9.50	9.01					
33.18	1.15	2.70	7.20						
47.61	0.96	1.91	9.05						
56.47	0.86	1.63	10.44						
59.19	1.15	1.56	7.93						
69.54	1.15	1.35	8.40						
76.80	0.96	1.24	10.56						

3.2 FT-IR analysis

FTIR spectrum is a useful tool used to determine the functional groups of products and their interactions with each other. FT-IR spectral data were obtained on a Perkin Elmer Spectrum 65 spectrophotometer equipment with an ATR-Kit system in the range of 4000–600 cm⁻¹ at room temperature. Fig. 3 presents a typical FT-IR spectra of PEG/PVP, PEG/PVP:CeO₂ and PEG/PVP:CeO₂:Er³⁺ (1-5wt.%), where the broadband around 3450 cm⁻¹ observed due to the hydrophilic character of PVP is attributed to the O–H stretching vibrations [26,27]. The stretching mode of vibration coinciding with C=C is obtained at 1652 cm⁻¹, and the alkyl group is also observed in the range of 2881–2955 cm⁻¹. The sharp vibrational band at 1654 cm⁻¹ is attributed to the stretching mode of the C=O in the PEG and PVP. The other important peak at 1423 cm⁻¹ is referring –CH deformation of cyclic CH₂ groups in the pyrrole ring of PVP. Another noticeable peak at 1285 cm⁻¹ can be related to C–N stretching mode of the amide group. The sharp and intense vibrational peaks that appeared at 1100, 952, and 841 cm⁻¹ are assigned to ring in-plane bending [28].

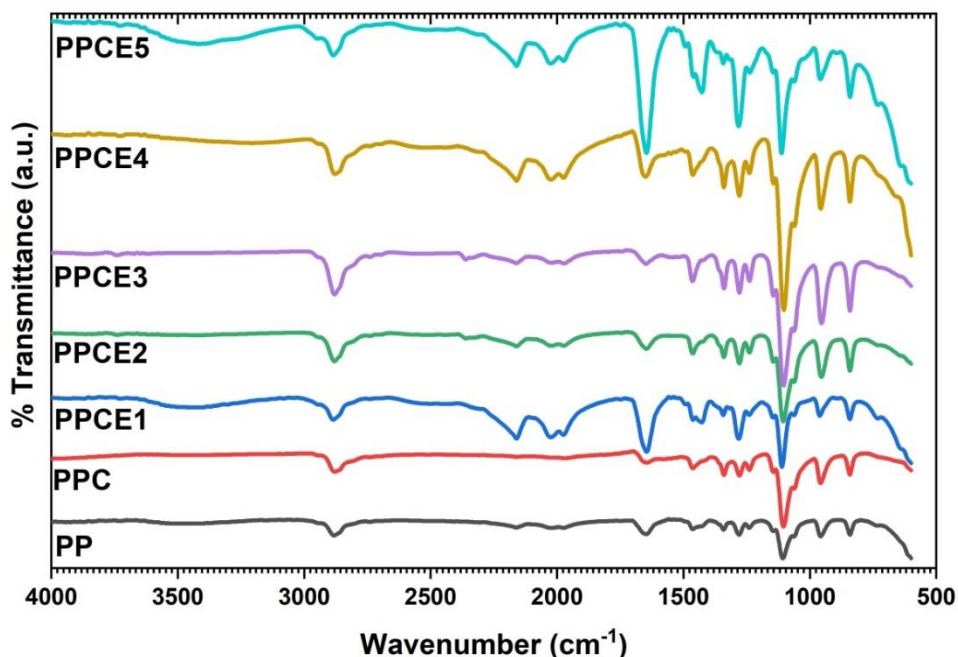


Fig. 3 FT-IR spectra of pristine-CeO₂, Peg/PVP:CeO₂ and PEG/PVP:CeO₂:Er³⁺(1-5wt.%).

Changing energy levels of O-H bonds, affected by the stretching frequencies of water molecules resulting from moisture on the surface of the sample, lead to a modification in the FTIR spectrum, resulting in an increase or decrease in band intensity. This phenomenon is likely a result of chemical interactions within the matrix triggered by dopant elements, resulting in structural and chemical changes visible in the FTIR spectrum. These data support the consistency of our results with the existing literature [29,30].

3.3 Luminescence Properties

Photoluminescence spectroscopy (PL) is a useful tool that provides insight into the role of electron pair recombination. Photoluminescence spectrum at room temperature excited by 349 nm wavelength of Nd:YLFQ switched pulse laser with tripled frequency for hybrid films that called PEG/PVP, PEG/PVP:CeO₂, PEG/PVP:CeO₂: xEr³⁺ (x=1-5wt%) is shown in Fig. 4. Figure 4a shows the solid-state luminescence spectrum of PEG/PVP polymer films with a blue light emission band in the range of 400–700 nm (centered at 515 nm). This broad emission band is attributed to $n \rightarrow \pi$ or $\pi \rightarrow \pi^*$ electronic transition (ILCT) [31–33].

Fig. 4b demonstrates the PL data for CeO₂-doped PEG/PVP-blended polymers. As noticed from the plot, concerning the PEG/PVA polymer mixture, the luminescence spectrum was blue-shifted by about 10 nm, and the PL intensity decreased by about three times with the CeO₂ doping in the sample matrix. The lowering in the PL intensity is likely due to the decrease in the recombination rate between electron and hole pairs, increasing the number of non-radiative defects in the blended polymer. Doping CeO₂ becomes new defect states that act as non-radiative centers. As a result, while nano-filler increases the number of defect states. the luminescence intensity decreases [34].

In Fig. 4c the PL emission spectra of PEG/PVP:CeO₂:xEr³⁺ (x=1-5wt%) consists of three main peaks at 536 (green emitted), 553 (green emitted) and 660 nm (red emitted), which is also attributed to transitions between $^5H_{11/2} \rightarrow ^4I_{15/2}$ (536 nm) states, $^4S_3 \rightarrow ^4I_{15/2}$ (553 nm)

states, ${}^4F_{9/2} \rightarrow {}^4I_{15/2}$ (660 nm), respectively. In addition to this weak emission peak observed in the NIR region at 1528 nm, which originated with the ${}^4I_{13/2} \rightarrow {}^4I_{15/2}$ transition (Fig 4d) [35–37]. In the spectral positions, there were no observed shifts. It is known that spectral positions of emission bands do not depend on the doping concentration and excitation mechanism. However, doping concentration seriously affects the luminescence intensity [38].

Fig. 4c and 4d illustrate that when the Er^{3+} doping concentration is increased, while the emission intensity is decreased. This decrease can be explained as follows:

- At low concentrations, $\text{Er}^{3+}-\text{Er}^{3+}$ ion distances are very far from each other and Er^{3+} ions are positioned randomly in the lattice.
- As the concentration increases, the distance between two Er^{3+} ions decreases considerably, resulting in the formation of Er^{3+} clusters.
- The excessive increase in concentration causes concentration-quenching processes in which dominant non-radiative transitions will occur.

Furthermore, the CIE values are (0.291; 0.360), (0.301; 0.329), (0.304; 0.334), (0.305; 0.323), (0.307; 0.321), (0.307; 0.317) and (0.306; 0.318) for PP, PPC, PPCE1, PPCE2, PPCE3, PPCE4 and PPCE5, respectively (Fig. 4e). Moreover, PEG/PVP: CeO_2 : Er^{3+} (1wt.%) is observed to broadband effect, which is due to the presence of polymer blend effects. As the Er^{3+} ion contribution in the (PVA-PEG) matrix increases. The narrow and sharp emission peaks are observed instead of a wide emission band, which can be explained energy transfer process (Fig. 4f). Firstly, the excitation energy is absorbed by the polymer blend. After that energy is transferred to CeO_2 nano-fillers. At the end, the energy is transferred from CeO_2 nano-fillers to doped Er^{3+} ions and is observed in narrow emission peaks.

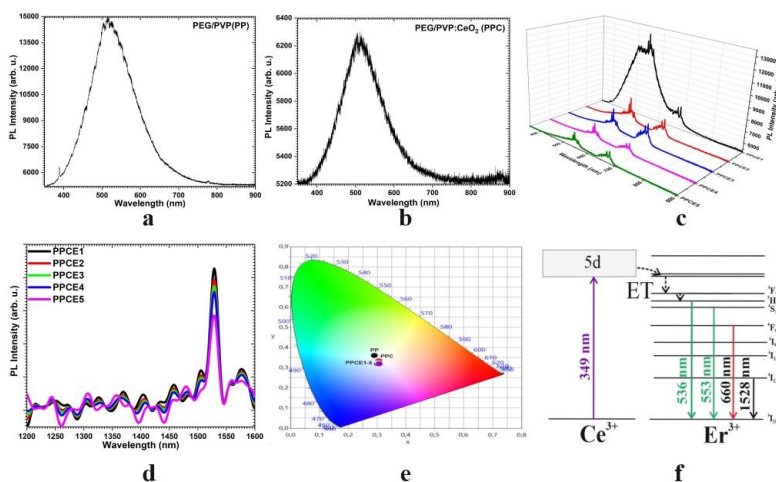


Fig. 3 The solid-state photoluminescence spectrum of hybrid film samples (a) PEG/PVP, (b) PEG/PVP: CeO_2 , (c) PEG/PVP: CeO_2 : $x\text{Er}^{3+}$ ($x=1-5\text{wt}\%$) in the visible region, (d) the solid-state emission spectra of the PEG/PVP: CeO_2 : $x\text{Er}^{3+}$ ($x=1-5\text{wt}\%$) films in the NIR region, (e) Chromaticity coordinates of all hybrid films and (f) Simplified energy level diagram of Ce^{3+} and Er^{3+} with arrows indicating optical transitions representing luminescence bands.

4. Conclusion

In this work, we present a facile method combined with the synthesis of copolymers and rare earth ions-doped CeO₂ NPs, and this technique allows the comparison of some physico-optical properties by varying the ratio between CeO₂:Er³⁺ and copolymer components. The pure CeO₂, CeO₂:Er³⁺ (x wt.%, x=1-5) nanocomposites and PEG/PVP, PEG/PVP:CeO₂, PEG/PVP:CeO₂:Er³⁺ (x wt.%, x=1-5) blended films were successfully synthesized by precipitation and solution casting technique, respectively. The XRD diffraction patterns revealed well-crystallized all samples and the average particle sizes of the pure CeO₂ and blended polymer film samples were established to be around 9.00-11.76 nm. Regarding the photoluminescence results, the green emission assigned to ⁴S_{3/2}→⁴I_{15/2} nm is dominant for PEG/PVP:CeO₂:Er³⁺ blended films. The predominant green emission implies that PEG/PVP:CeO₂:Er³⁺ hybrid films can be used as potential green luminescent materials.

Additionally, a weak emission peak was observed at 1528 nm, assigned to ⁴S_{3/2}→⁴I_{15/2}. Considering the optical performance in the NIR region, Er³⁺ doped hybrid films may be candidates for potential materials that can be used in NIR OLEDs. The results of the study pave the way for many suggestions and, accordingly, the production of new ideas and more detailed research.

References

1. Abdelrazek EM, Elashmawi IS, El-khodary A, Yassin A. Structural, optical, thermal and electrical studies on PVA/PVP blends filled with lithium bromide. *Curr. Appl. Phys*, 2010;10:607–613.
2. Alam TM, Otaigbe J, Rhoades D, Holland G, Cherry B, Kotula P. Nanostructured polymer blends: Synthesis and structure. *Polymer*, 2005;46:12468–12479.
3. Baskaran R, Selvasekarapandian S, Kuwata N, Kawamura J, Hattori T. Conductivity and thermal studies of blend polymer electrolytes based on PVAc-PMMA. *Solid State Ionics*, 2006;177: 2679–2682.
4. Demir MM, Memesa M, Castignolles P, Wegner G. PMMA/Zinc Oxide Nanocomposites Prepared by In-Situ Bulk Polymerization. *Macromol. Rapid Commun*, 2006;27:763–770.
5. Kumar K, Ravi M, Pavani Y, Bhavani S, Sharma A, Narasimha Rao V. Investigations on PEO/PVP/NaBr complexed polymer blend electrolytes for electrochemical cell applications. *J. Memb. Sci*, 2004; 454: 200–211.
6. Kumar N, Acharya S, Alhadhrami A, Prasanna B, Gurumurthy S, Bhat S. Role of TiO₂/ZnO Nanofillers in Modifying the Properties PMMA Nanocomposites for Optical Device Applications. *Iran. J. Sci. Technol. Trans. A Sci*, 2021;45:2169–2179.
7. Alzahrani HAH. CuO and MWCNTs Nanoparticles Filled PVA-PVP Nanocomposites: Morphological, Optical, Thermal, Dielectric, and Electrical Characteristics. *J. Inorg. Organomet. Polym. Mater*, 2022;32:1913–1923.
8. Badry R, Fahmy A, Ibrahim A, Elhaes H, Ibrahim M. Application of polyvinyl alcohol/polypropylene/zinc oxide nanocomposites as sensor: modeling approach. *Opt. Quantum Electron*, 2021;53:39.
9. Heiba ZK, Mohamed MB, El-naggar AM, Altowairqi Y, Kamal AM. Impact of ZnCdS/M (M = Co, Fe, Mn, V) doping on the structure and optical properties of PVA/PVP polymer. *J. Polym. Res*, 2021;28:472.
10. Heiba ZK, Bakr Mohamed M, Ahmed SI. Exploring the physical properties of PVA/PEG polymeric material upon doping with nano gadolinium oxide. *Alexandria Eng. J*, 2022;61:3375–3383.

11. Kusmierek E. A CeO₂ Semiconductor as a Photocatalytic and Photoelectrocatalytic Material for the Remediation of Pollutants in Industrial Wastewater: A Review. *Catalysts*, 2020;10:1435.
12. Wang F, Wei M, Evans DG, Duan X. CeO₂ -based heterogeneous catalysts toward catalytic conversion of CO₂. *J. Mater. Chem. A* 2016;4:5773–5783.
13. Singhania N, Anumol EA, Ravishankar N, Madras G. Influence of CeO₂ morphology on the catalytic activity of CeO₂-Pt hybrids for CO oxidation. *Dalt. Trans*, 2019;42:15343.
14. Leino E, Kumar N, Maki-Arvela P, Aho A, Kordas K, Leino AR, Shchukarev A, Murzin DY, Mikkola JP. Influence of the synthesis parameters on the physico-chemical and catalytic properties of cerium oxide for application in the synthesis of diethyl carbonate. *Mater. Chem. Phys*, 2013;143:65–75.
15. Tsunekawa S, Sahara R, Kawazoe Y, Kasuya A. Origin of the Blue Shift in Ultraviolet Absorption Spectra of Nanocrystalline CeO_{2-x} Particles. *Mater. Trans. JIM*, 2000;41:1104–1107.
16. Vivier L, Duprez D. Ceria-Based Solid Catalysts for Organic Chemistry. *ChemSusChem*, 2010;3:654–678.
17. Garzon F. Solid-state mixed potential gas sensors: theory, experiments and challenges. *Solid State Ionics*, 2000;136–137:633–638.
18. Bekyarova E, Fornasiero P, Kašpar J, Graziani M. CO oxidation on Pd/CeO₂-ZrO₂ catalysts. *Catal. Today*, 1998;45:179–183.
19. Wang W, Wang S, Ma X, Gong J. Crystal structures, acid–base properties, and reactivities of CexZr1-xO₂ catalysts. *Catal. Today*, 2009;148:323–328.
20. Ropuszyńska-Robak P, Macalik L, Lisiecki R, Hanuza J. Luminescence behaviour of the synthesized erbium and thulium co-doped potassium, sodium, lithium or rubidium yttrium double tungstate nanopowders. *Opt. Mater*, 2020;110:110459.
21. Artizzu F, Mercuri ML, Serpe A, Deplano P. NIR-emissive erbium–quinolinolate complexes. *Coord. Chem. Rev*, 2011;255:2514–2529.
22. GhaedRahmati H, Frounchi M, Dadbin S. Piezoelectric behavior of Gamma-radiated nanocomposite hydrogel based on PVP-PEG-BaTiO₃. *Mater. Sci. Eng*, 2022;B276:115535.
23. Saroj AL, Singh RK, Chandra S. Studies on polymer electrolyte poly(vinyl) pyrrolidone (PVP) complexed with ionic liquid: Effect of complexation on thermal stability, conductivity and relaxation behaviour. *Mater. Sci. Eng*, 2013;B178:231–238.
24. Barron MK, Young TJ, Johnston KP, Williams RO. Investigation of processing parameters of spray freezing into liquid to prepare polyethylene glycol polymeric particles for drug delivery. *AAPS PharmSciTech*, 2003;4:1–13.
25. Kumar N, Verma S, Park J, Chandra Srivastava V, Naushad M. Evaluation of photocatalytic performances of PEG and PVP capped zinc sulfide nanoparticles towards organic environmental pollutant in presence of sunlight. *Chemosphere*, 2022;298:134281.
26. Yahsi Y, Gungor E, Coban MB, Kara H. Linear trinuclear mixed valence Mn III -Mn II -Mn III complex: Synthesis, crystal structure and characterization. *Mol. Cryst. Liq. Cryst*, 2016;637:67–75.
27. Coban MB, Gungor E, Kara H, Baisch U, Acar Y. New mixed valence defect dicubane cobalt(II)/cobalt(III) complex: Synthesis, crystal structure, photoluminescence and magnetic properties. *J. Mol. Struct*, 2018;1154:579–586.
28. Zhang B, Zhang L, Li J, Fu J, Qu X. Fabrication of Zr-MOF filled PVA/CS blended membranes for high efficiency CO₂ separation. *J. Ind. Eng. Chem* 2023;133:148–161.

29. Yousaf AM, Malik UR, Shahzad Y, Mahmood T, Hussain T. Silymarin-laden PVP-PEG polymeric composite for enhanced aqueous solubility and dissolution rate: Preparation and in vitro characterization. *J. Pharm. Anal*, 2019;9:34–39.
30. Ebadi A, Rafati AA, Bavafa S, Mohammadi M. Kinetic and theoretical studies of novel biodegradable thermo-sensitive xerogels based on PEG/PVP/silica for sustained release of enrofloxacin. *Appl. Surf. Sci*, 2017;425:282–290.
31. Gungor E, Coban MB, Kara H, Acar Y. Antiferromagnetic Coupling in a New Mn(III) Schiff Base Complex with Open-Cubane Core: Structure, Spectroscopic and Luminescence Properties. *J. Clust. Sci*, 2018;29:533–540.
32. Gungor E, Coban MB, Kara H, Acar Y. Photoluminescence and Magnetism Study of Blue Light Emitting the Oxygen-Bridged Open-Cubane Cobalt(II) Cluster. *J. Clust. Sci*, 2018;29:967–974.
33. Acar Y, Kara H, Gungor E, Coban MB. Catena-Poly[[[2,4-dichloro-6-[[2-hydroxyethyl]imino]methyl]phenolato- κ ,3N,O,O']-copper(II)]- μ -chlorido] monohydrate]: Synthesis, structural, spectroscopic and luminescent properties. *Mol. Cryst. Liq. Cryst*, 2018;664:165–174.
34. El-naggar AM, Heiba ZK, Mohamed MB, Kamal AM, Lakshminarayana G. Thermal, linear and nonlinear optical properties of PVA/PVP/PEG blends loaded with nanovanadium-doped nano tin disulfide. *J. Mater. Sci. Mater. Electron*, 2022;33:25743–25752.
35. Acar Y, Coban MB, Gungor E, Kara H. Two New NIR Luminescent Er(III) Coordination Polymers with Potential Application Optical Amplification Devices. *J. Clust. Sci*, 2020;31:117–124.
36. Erkarlan U, Donmez A, Kara H, Aygun M, Coban MB. Synthesis, Structure and Photoluminescence Performance of a New Er³⁺-Cluster-Based 2D Coordination Polymer. *J. Clust. Sci*, 2018;29:1177–1183.
37. Tamrakar RK, Bisen DP, Brahme N, Sahu IP, Upadhyay K. Structural and luminescence behavior of Gd₂O₃:Er³⁺ phosphor synthesized by solid state reaction method. *Optik*, 2015;126:2654–2658.
38. Kolesnikov IE, Mamonova DV, Koruchkin MA, Medvedev VA, Bai G, Kolesnikov EY. Structural, luminescence and thermometric properties of LaVO₄:Ln³⁺ nanopowders (Ln=Dy and Sm). *J. Alloys Compd*, 2023;965:171388.